WILEY InterScience® DISCOVER SOMETHING GREAT

DFT Study of Rearrangements in Cyclopentylheptenyl Carbocations

VALERIJE VRCEK

Faculty of Pharmacy and Biochemistry, University of Zagreb, A. Kovacica 1, 10000 Zagreb, Croatia

Received 15 August 2006; accepted 4 October 2006
Published online 15 November 2006 in Wiley InterScience (www.interscience.wiley.com).
DOI 10.1002/qua.21258

ABSTRACT: Carbocation rearrangements relevant to sterol biosynthesis were investigated computationally by using the model cyclopentylheptenyl carbocations **1A** and **1B**. Five different rearrangement pathways of these equilibrating cations were located at the potential energy surface (PES), all calculated at the B3LYP/6-31G(*d*) level of theory. Each of these five distinct pathways differs from previous mechanistic proposals, and each involves new and unusual intermediates. © 2006 Wiley Periodicals, Inc. Int J Quantum Chem 107: 1772–1781, 2007

Key words: DFT calculation; carbocation; sterol biosynthesis; reaction mechanism; biomimetic rearrangement

Introduction

It is well established that all steroid hormones and triterpenoids arise from 2,3-epoxysqualene in enzymatic polycyclization reactions [1]. After the introduction of the idea of a stepwise mechanism of biomimetic olefin cyclization via conformationally flexible carbocationic intermediates [2], attention has focused on each step of the cyclization. Both experimental and quantum chemical investigations were undertaken to determine a detailed mechanism and energetics underlying the cyclization steps. In the quantum chemical approach, different model systems are used for the biomimetic study of the corresponding cyclization reactions [3]. Of special importance are cyclopentylheptenyl cation models, which comprise both carbocationic and olefinic moieties. Such substrates are appropriate to model cation–olefin cascades, particularly the formation of the four rings (A–D).

In a recent report, a mechanism for simultaneous C-ring expansion and D-ring formation in lanosterol biosynthesis was proposed [4]. This mechanism involves the model 2-cyclopentyl-6-methyl-2-hept-5-enyl carbocation (**1A**), which undergoes a concerted ring expansion and ring closure, via the bridged transition state structure **TS1**, to give the bicyclo [4.3.0]nonyl tertiary carbocation **2** (Scheme 1).

Such a rearrangement would avoid the intermediacy of the unstable secondary cyclohexyl cation, as well as violation of Markovnikov's rule. At the

Correspondence to: V. Vrcek; e-mail: valerije@pharma.hr
Contract grant sponsor: Ministry of Science, Education and Sports of the Republic of Croatia.
Contract grant number: 0006451.

© 2006 Wiley Periodicals, Inc.

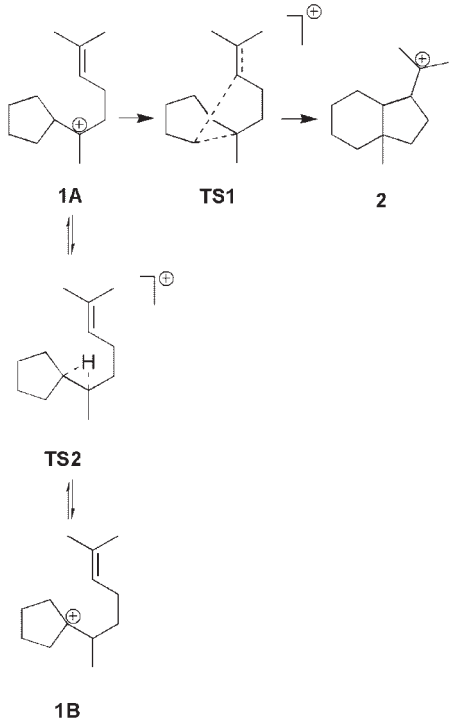

SCHEME 1. Ring enlargement and 1,2-hydride shift processes in the carbocation **1A**.

B3LYP/6-31G(*d*) level, the energy barrier of 7.8 kcal/mol has been calculated for this rearrangement **1A** → **2** [4].

For comparison, in the rearrangement of the 2-(2,2,3-trimethylcyclopentyl)-2-propyl cation, the energy barrier required to expand this model tertiary cyclopentyl carbocation (Scheme 2) [3a,b] to the less stable secondary cyclohexyl cation (1,1,2,2,3-pentamethyl-6-cyclohexyl cation) is ~5–6 kcal/mol higher than the barrier for the rearrangement **1A** → **2**. However, structures involved in that ring expansion reaction were calculated only at the Hartree–Fock (HF)/6-31G(*d*) level of theory. At both the density functional theory (DFT) and second-order Møller–Plesset (MP2) levels, it has been found that the secondary structure of the 1,1,2,2,3-pentamethyl-6-cyclohexyl cation is not a minimum,

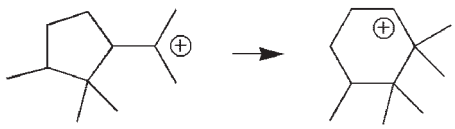

SCHEME 2. Ring enlargement of the 2-(2,2,3-trimethylcyclopentyl)-2-propyl cation.

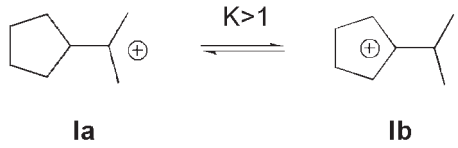

SCHEME 3. 1,2-hydride shift in the 2-cyclopentyl-2-propyl cation.

but it is converged to the corresponding tertiary cyclohexyl cation via an intramolecular methyl shift [5]. Hence, it is proposed that the biomimetic cascade arising from the protonation of squalene epoxide could occur without the necessity of going through the higher-energy intermediate secondary carbocation. To provide computation for this hypothesis, the ring expansion process **1A** → **2** has been employed as a suitable model reaction.

However, our earlier experimental and quantum chemical results [6] on the corresponding model 2-cyclopentyl-2-propyl cation (**Ia** in Scheme 3), which is structurally related to cation **1A**, suggest that other possible (and more favorable) rearrangement mechanisms for the model carbocation **1A** should be considered. In addition, we have found that the computational results related to the model cyclopentylcarbinyl carbocation **1A** are sensitive both to the substituent (see, e.g., Ref. [7]) and solvent effects and to the level of theory employed (see below, and see, e.g., Ref. [8]). In the present work, we present several other mechanisms for the rearrangement of the cyclopentylcarbinyl carbocation **1A**, which are relevant to sterol biosynthesis.

Computational Methods

The quantum chemical calculations were performed using the Gaussian 03 program suites [9]. All structures were fully optimized using DFT hybrid methods with the B3LYP functional [10]. The standard split valence and polarized 6-31G(*d*) basis set was used for geometry optimizations and frequency calculations. Optimized coordinates of all structures are included in the Supporting Information. Analytical vibrational analysis at the same level were performed to determine the zero-point vibrational energy (ZPE) and to characterize each stationary point as a minimum (Nimag = 0) or first-order saddle point (Nimag = 1). IRC calculations (intrinsic reaction coordinate as implemented in Gaussian 03) were performed at the B3LYP/6-

31G(*d*) level. The initial geometries used were that of the corresponding transition states structures, and the paths were followed in both directions from that point. This method verified that a given transition structure indeed connected the presumed energy minimum structures [11]. Corrections for ZPE (not scaled) are included in the calculated energies. A more complete treatment of electron correlation was made by performing MP4(SDTQ)/6-31G(*d*) single-point energy calculations for some structures (**1A**, **1B**, **2**, **3**, **4**, **5**, **6**, **TS1**, **TS6**, and **TS6'**) optimized at the MP2/6-31G(*d*) level. The inclusion of MP4 correlation energy correction is necessary to correctly estimate the relative energy differences for carbocations involved in the processes under study. The relative energies are given in kcal/mol with respect to the carbocation **5** and are listed in Table I.

Results and Discussion

It is shown that the model carbocation **Ia** is not static in solution, but undergoes rapid nondegenerate hydride shift over the low-energy barrier (Scheme 3), interchanging the 2-cyclopentyl-2-propyl cation (**Ia**) and the 1-(2-propyl)cyclopentyl cation (**Ib**). Experimental and quantum chemical studies have indicated that the equilibrium is shifted toward the 1-(2-propyl)cyclopentyl cation (**Ib**), in which the positive charge is located in the ring [6]. The carbocation **Ia**, in which positive charge is located out of the ring, was found to be ~1.5 kcal/mol less stable than the carbocation **Ib**, in which positive charge is located in the ring [6]. In this study, we demonstrate the computational evidence that the similar applies to the model cyclopentylcarbinyl carbocation **1A**. At the B3LYP/6-31G(*d*) level of theory, the cyclopentylcarbinyl carbocation **1A**, in which the positive charge is located out of the ring, was calculated 1.2 kcal/mol less stable (Table I) than the carbocation **1B** with a positive charge located in the ring (Scheme 1). This more stable isomeric cyclopentylheptenyl carbocation **1B** has not been described earlier. It has a conformation favorable for the β-CC–hyperconjugative interaction between the C2-methyl group and a formally vacant $2p\pi$ orbital at the endocyclic carbon C1 (Fig. 1). The two isomers, **1A** and **1B**, undergo rapid hydride shift via the transition state structure **TS2**. It is a hydrido-bridged transition structure (Fig. 2) characterized by an unsymmetrical C—H—C bond (C1—H is 1.373 Å, and C2—H is 1.330 Å at the B3YLP-6-31G(*d*) level), while the C1—C2 bond length is shortened to 1.403 Å as compared with the averaged single C—C bond length. The only imaginary frequency ($418i$ cm^{-1}) corresponds to the hydride shift between C1 and C2 carbon atoms. At the B3LYP/6-31G(*d*) level, this transition structure was calculated ~4 kcal/mol less in energy than the transition state structure **TS1**, which suggest that the hydride shift process **1A** → **1B** is energetically more favorable than the ring enlargement process **1A** → **2**. Therefore, instead of structure **1A**, structure **1B** should be considered as a starting point for the corresponding cyclization process in which the carbocation **2** is formed. This means that the calculated energy barrier for the overall ring expansion process **1B** → **2** (Scheme 1) is 10.6 kcal/mol (Table I). As well, we assume that the carbocation **1B** is a better candidate to study rearrangement mechanisms relevant to steroid biosynthesis. Indeed, it was shown by Epstein that the 2-methyl-6-(1-hydroxycyclopentyl)-2-heptene (**B**), which is an alcohol precursor of the carbocation **1B**, undergoes an acid catalyzed cyclization to give 1-isopropyl-7-methylbicyclo[4.3.0]non-6-ene (**C**) in greater than 95% isolated yield (Scheme 4) [12]. This experimental result is consistent with the intermediacy of the carbocation **1B** and spiro carbocations **3** and **4**, as well as the carbocation **5**. The 2-methyl-6-cyclopentyl-6-hydroxy-2-heptene (**A**), which is an alcohol precursor of the carbocation **1A**, also forms the 1-isopropyl-7-methylbicyclo[4.3.0]non-6-ene (**C**) in high yield which means that an initial fast 1,2-hydride shift **1A** → **1B** (see Scheme 1) via **TS2** must occur prior to any cyclization process.

There are several possible mechanisms for the rearrangement of the carbocation **1B**. We have considered rearrangements which are consistent with the experimental results and which involve carbocation intermediates important for sterol biosynthesis. The first rearrangement discussed is related to the experimental work in which Epstein et al. [12] postulated that acid dehydration of the 2-cyclopentyl-6-methylhept-5-en-2-ol (**A**) and/or the 1-(6-methylhept-5-en-2-yl)cyclopentanol (**B**) gives rise to tertiary carbocation intermediate **5** (Scheme 4). At the B3LYP/6-31G(*d*) level, the final carbocation product **5** was calculated to be 11.5 kcal/mol more stable than the bicyclo[4.3.0]nonyl carbocation **2**, the final product of the rearrangement process proposed by Hess (Scheme 1). The carbocation **1B** undergoes five-membered ring closure, via the transition state structure **TS3**, to give the spiro-type

TABLE I

Total energies, relative energy differences,[a] and number of imaginary frequencies calculated for structures involved in rearrangements of cyclopentylheptenyl carbocations 1A and 1B.

Structure	B3LYP/6-31G(*d*) [MP4/6-31(*d*)][b]	Δ*E* (kcal/mol)	NImag[c] (ν/cm^{-1})
1A[d]	−508.963068	13.4	0
	(−507.091882)	(22.5)	
1B	−508.965565	12.2	0
	(−507.094422)	(20.9)	
2	−508.969206	11.5	0
	(−507.132934)	(3.2)	
3	−508.964782	13.4	0
	(−507.115918)	(7.5)	
4	−508.979218	4.9	0
	(−507.127556)	(0.2)	
5	−508.984457	0	0
	(−507.127831)	(0)	
6	−508.978115	3.2	0
	(−507.123813)	(2.5)	
7	−508.984905	0.9	0
8[e]	−508.928699	33.2	0
9	−508.934497	30.6	0
10	−508.967969	11.7	0
11	−508.950082	21.0	0
TS1	−508.948311	22.8	1
	(−507.091161)	(24.1)	(247*i*)
TS2	−508.950904	19.0	1
			(418*i*)
TS3	−508.964203	13.7	1
			(127*i*)
TS4	−508.953581	19.3	1
			(405*i*)
TS5	−508.972625	9.5	1
			(202*i*)
TS6	−508.934326	31.2	1
	(−507.085641)	(25.8)	(427*i*)
TS6′	−508.927773	35.2	1
	(−507.077371)	(31.7)	(654*i*)
TS7	−508.973919	8.3	1
			(166*i*)
TS8	−508.927111	37.6	1
			(370*i*)
TS9	−508.925544	36.1	1
			(499*i*)
TS10	−508.962382	13.8	1
			(74*i*)
TS11	−508.947228	23.5	1
			(39*i*)

[a] Relative energies (ZPE included) with respect to the most stable carbocation structure **5.**

[b] Single-point energy calculations at the MP4/6-31G(*d*)//MP2/6-31G(*d*) level.

[c] B3LYP/6-31G(*d*) values.

[d] The calculated structure of **1A** is 1.6 kcal/mol more stable than its conformer reported earlier by Hess [4].

[e] The secondary carbocation **8** can be considered as either an artifact structure or transition state structure because, at the MP2/6-31G(*d*) level of theory, it does not exist as a minimum.

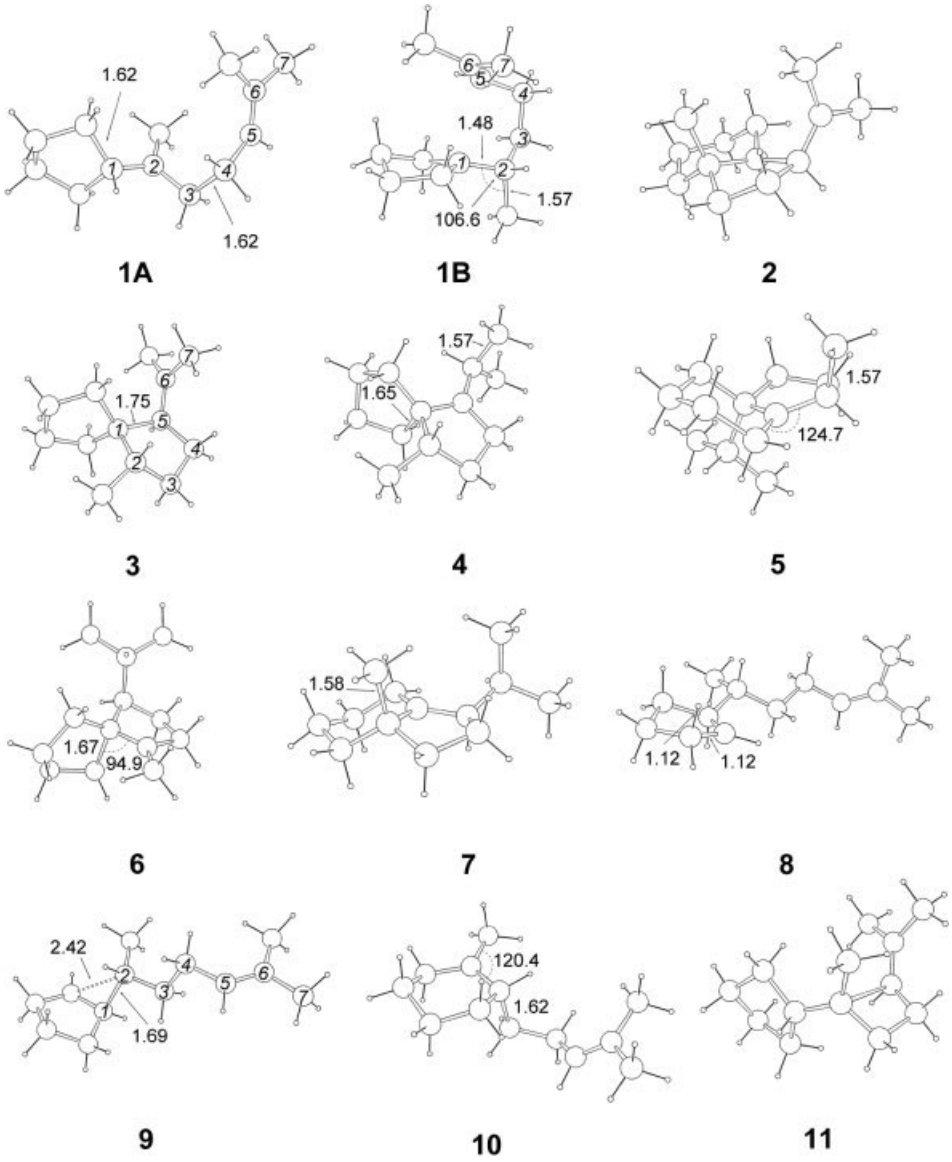

FIGURE 1. B3LYP/6-31G(*d*) optimized geometries of intermediates involved in rearrangements of cyclopentylheptenyl type of carbocations. Bond lengths are in Ångstroms (Å), and angles are in degrees (°).

carbocation **3**. The transition state structure **TS3** is calculated only 1.5 kcal/mol less stable than the reactant **1B** (Table I), and is characterized by one imaginary frequency (127*i* cm^{-1}), which correspond to the formation of the C1—C5 bond (the calculated distance of 2.144 Å in Fig. 2). Spiro-type carbocations **3** and **4** are interconnected via the hydrido-bridged transition state **TS4** (405*i* cm^{-1}), which is a rate determining transition state structure (the least stable transition state structure) for the rearrangement pathway presented in Scheme 4. Similarly to the geometry of **TS2**, the transition state structure **TS4** is characterized by unsymmetrical three-center two-electron C—H—C bond (Fig. 2). In this case of spiro-type carbocations it is found again that the isomer **4**, having positive charge in the ring, is more stable (8.5 kcal/mol at the B3LYP/6-31G(*d*) level) than the isomer **3**, which has a positive charge on the exocyclic carbon. Both isomers, **3** and **4**, are β-CC-hyperconjugatively stabilized carbocations with elongated C—C bonds involved in hyperconjugation (Fig. 1). The carbocation **5**, the most stable intermediate in the corresponding rearrangement process (Table I), is easily formed from

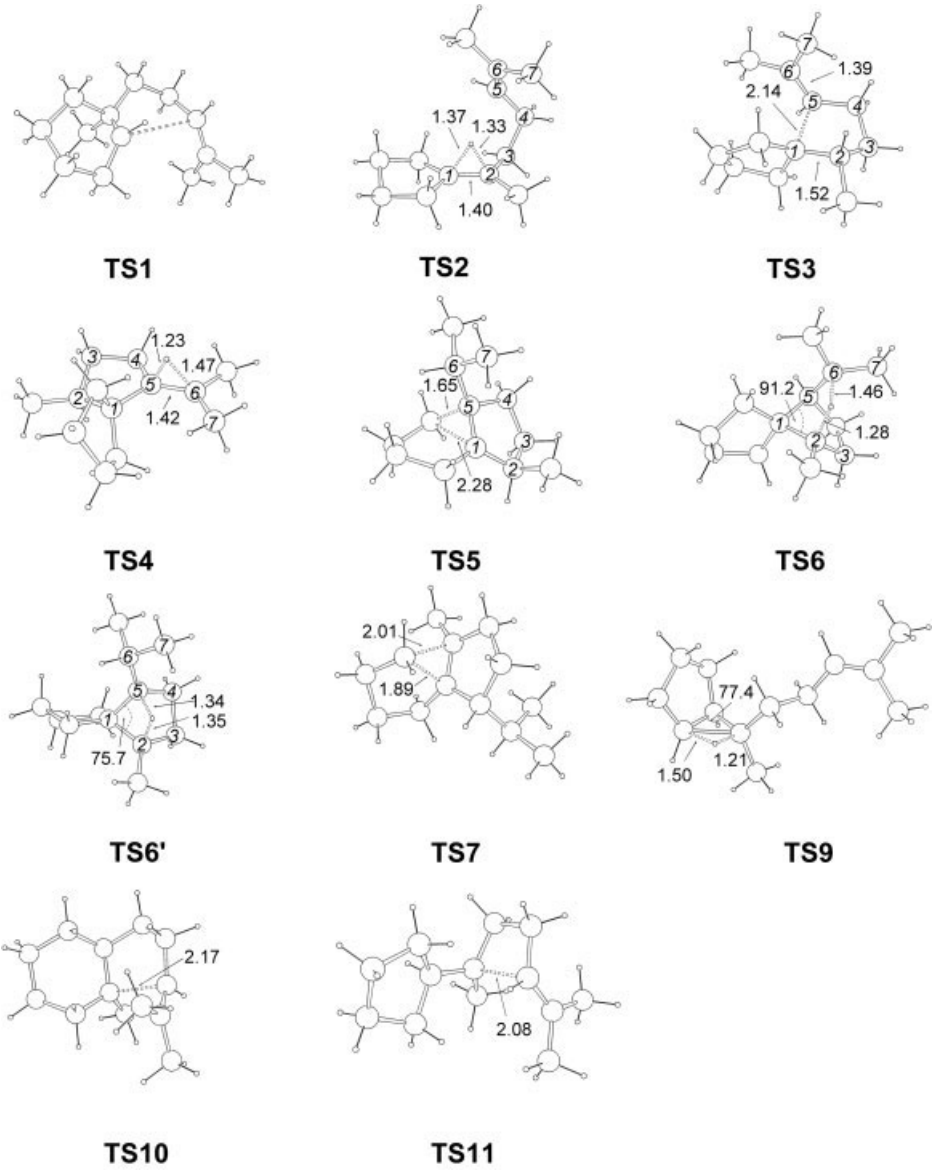

FIGURE 2. B3LYP/6-31G(*d*) optimized geometries of transition state structures involved in rearrangements of cyclopentylheptenyl type of carbocations. Bond lengths are in Ångstroms (Å), and angles are in degrees (°).

the spiro cation **4** via the transition state structure **TS5**. The only imaginary frequency (202*i* cm^{-1}) is associated with the elongation of one C—C bond (the calculated distance of 2.281 Å in Fig. 1) and simultaneous formation of another C—C bond (the calculated distance of 1.653 Å). The calculated overall energy barrier for the ring enlargement **1B** → **5** (Scheme 4) is 7.1 kcal/mol, which is for 3.5 kcal/mol lower that the barrier for the formation of the carbocation **2** (Scheme 1). Thus, the rearrangement of the carbocation **1B**, via transition state structure **TS4** (Scheme 4), to the carbocation **5** is both thermodynamically and kinetically more favorable process than the rearrangement of carbocation **1B**, via transition state structure **TS1** (Scheme 1), giving the carbocation **2**. It is in accord with the experimental results presented above. The results obtained also indicate that the spiro-type carbocations (of type **3** and **4**) should be considered as important intermediates in this type of rearrangements. Indeed, on the basis of enzymic experiments on the 2,3-oxidosqualene, van Tamelen et al. [13] proposed earlier the biosynthetic route in which a lanosterol skeleton is produced via [5.5]-spiro intermediates.

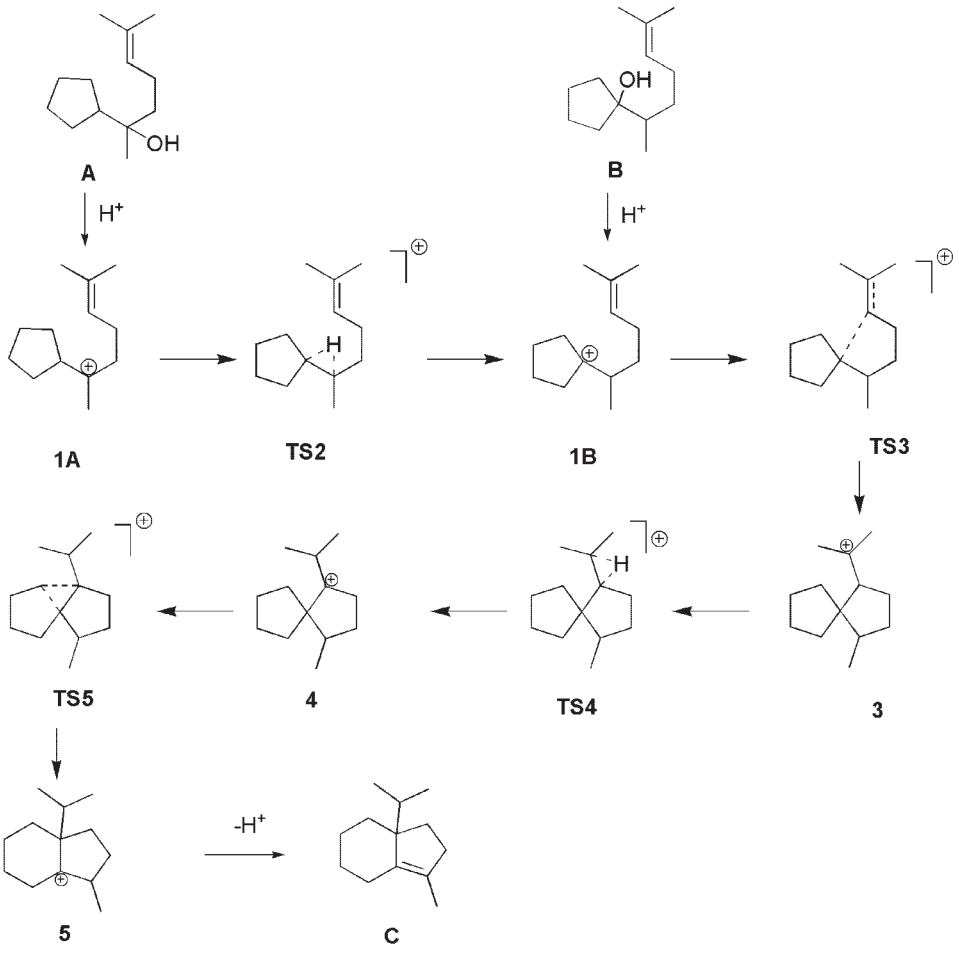

SCHEME 4. Mechanism of the acid catalyzed dehydration of cyclopentylheptenes **A** and **B**.

While the process **1B** → **5** (Scheme 4) yields an intermediate (indenyl cation **5**), which is not important to the biosynthesis of lanosterol, we have tested another possible rearrangement of carbocation **1B** in which both the spiro-intermediates of type **3** and **4** and the appropriate model bicyclo[4.3.0]nonyl carbocation **2** are involved (Scheme 5). In this pathway the spiro-carbocation **3** undergoes 1,4-hydride shift giving the spiro-carbocation **6**. Distant hydride shifts in spiro-type intermediates were suggested by van Tamelen and colleagues as alternative processes which are completely consistent with the body of biochemical tracer experiments [13, 14]. In the case of the squalene epoxide cyclization, van Tamelen's group proposed the 1,3-hydride shift as a more favorable process. However, we have calculated, at the B3LYP/6-31G(*d*) and MP2/6-31G(*d*) level, that the 1,3-hydride shift in the model reaction **4** → **6** is for ~4 kcal/mol less favorable process than the corresponding 1,4-hydride shift in the model reaction **3** → **6**. This is mostly due to unfavorable ring strain in the transition state structure **TS6′** (the calculated bond angle of 75.7° in Fig. 2). The transition state structure **TS6** for the 1,4-hydride shift is located at the B3LYP/6-31G(*d*) and MP2/6-31G(*d*) levels and is characterized by unsymmetrical C—H—C bridging. The only imaginary frequency (427*i* cm^{-1} at the DFT level) is associated with the movement of the bridging hydrogen atom between the two neighboring carbons. The ring enlargement process in the spiro-carbocation **6**, via the transition state structure **TS7** (Fig. 2), yields the indenyl carbocation **7**. The cation **7** is then easily converted to the final carbocation product **2** via subsequent low-energy barrier hydrogen migrations already reported experimentally by van Tamelen et al. [15]. The calculated energy barrier for the ring expansion process

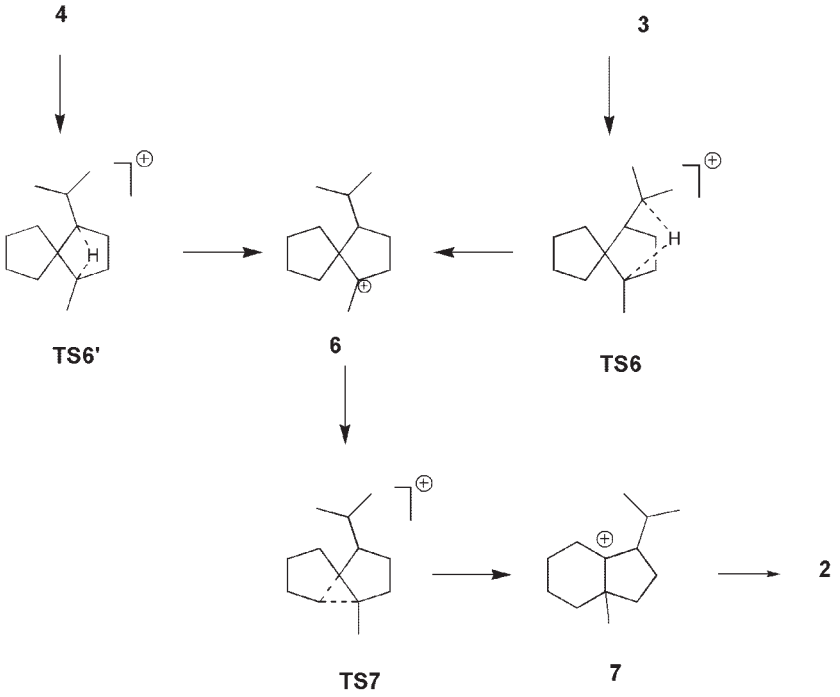

SCHEME 5. 1,3- and 1,4-hydride shifts in spiro-type carbocations **3** and **4**.

6 → **7** via the transition state structure **TS7** is for ~20 kcal/mol lower than the calculated barrier for the 1,4-hydride shift **3** → **6**. Thus, the overall energy barrier, calculated at the DFT level, for the rearrangement pathway **3** → **7** (→ **2**) is 17.8 kcal/mol. The calculated energy barrier for the alternative rearrangement **1A** → **2** proposed by Hess [4] is only 9.5 kcal/mol. However, at our final level, i.e., MP4/6-31G(*d*)//MP2/6-31G(*d*), the calculated relative energy difference between the transition state structures **TS1** (rearrangement **1A** → **2** in Scheme 1) and **TS6** (rearrangement **3** → **7** in Scheme 5) is only 1.7 kcal/mol which suggests that these two rearrangements could be competitive. It is recently shown that the electron correlation using MP*n* methods is superior to B3LYP DFT hybrid methods for structures with hypercoordinated hydrogens involved in C—H—C bonds [16]. Therefore, MP4/6-31G(*d*) single-point energy calculation for the MP2/6-31G(*d*) optimized structures of **TS1** and **TS6** were performed to account for a more complete treatment of correlation and more accurate relative energies.

The third possible rearrangement pathway of carbocation **1B** involves the four energy minima (**1B**, **8**, **9**, and **10**) separated by three barriers (Scheme 6). However, at the MP2/6-31G(*d*) level of theory, the secondary carbocation structure **8** vanished from the corresponding potential energy surface (PES) and converged to the structure **9**. Therefore, the corner-protonated cyclopropane intermediate **9** can be formed directly from **1B** by an uphill 1,2-hydride migration and simultaneous 1,2-isopropyl shift. The structure **9** contains the protonated cyclopropane moiety characterized by both elongated CC bonds and partial bridging (Fig. 1). Corner-to-corner hydride shift in **9**, with simultaneous C—C bond cleavage leads, via the transition state **TS9**, to the cyclohexyl type of carbocation **10**. This intermediate undergoes ring closure, via the transition state structure **TS10**, giving the final product **2**. The highest stationary point at the PES of this rearrangement pathway (Scheme 6) is the transition state structure **TS9**, which connects intermediates **9** and **10**. Whereas the minimum structure **9** is characterized by a corner-protonated cyclopropane moiety, the transition state structure **TS9** is characterized by an edge-protonated cyclopropane ring (Fig. 2). The rearrangement **9** → **10** is analogous to the rearrangement pathway of the model 1-(2-propyl)cyclopentyl cation reported earlier by Vrcek et al. [6]. Although the rearrangement **1B** → **10** is energetically less favorable than the three processes described earlier in this paper, it is of special

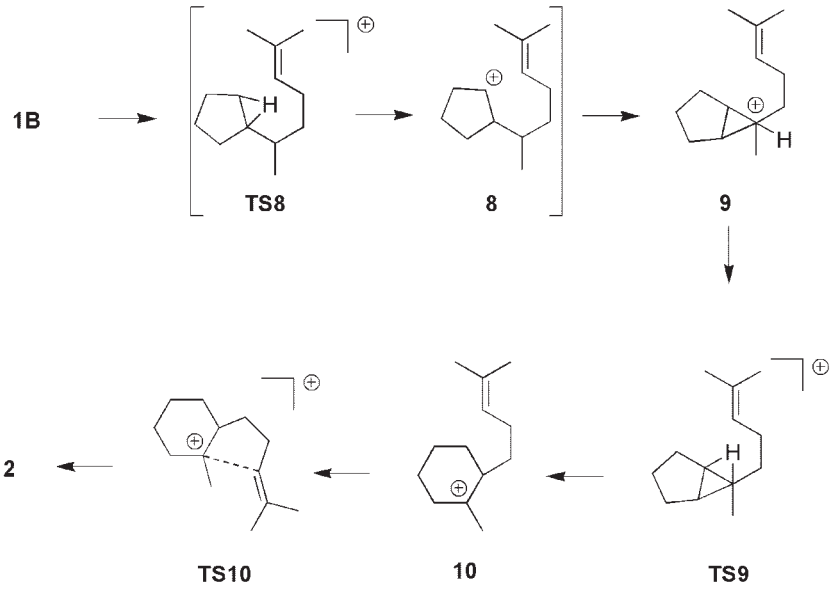

SCHEME 6. Rearrangement of **1B** → **2** involves protonated cyclopropane intermediates.

interest due to the intermediacy of the protonated cyclopropane intermediates (structures **9** and **TS9**). Several investigators proposed protonated cyclopropanes as key intermediates in different mono- and polycyclization reactions [17]. As well, quantum chemical calculations for cyclohexyl and methylcyclohexyl cations reported by Lee and Houk [18] show that substituted protonated cyclopropane play the central role in the outcome of cation–olefin cyclization.

Currently, we are exploring the rearrangement pathway in which, instead of the ring expansion process, the four-membered ring closure in **1A** takes place (Scheme 7). This mechanism is related to the enzymatic cyclization in which the didemethyloxidosqualene is predominantly converted into the product with 6-6-5 fused A–B–C ring system and a pendant four-membered "D"-ring [1, 19]. This unique cyclization is most easily explained by internal trapping of the carbocation intermediate **1A** through the intramolecular reaction with the electron-rich CC double bond. The transition state structure **TS11** (Fig. 2) for this ring closure process was located at B3LYP/6-31G(*d*) level. It is calculated 10.1 kcal/mol higher in energy than the carbocation **1A**, whereas the carbocation product **11**, with the pendant cyclobutyl ring (Fig. 1), is ~8 kcal less stable than **1A** (Table I). It comes out, as expected, that the four-membered "D" ring formation is both thermodynamically and kinetically unfavorable process unless the enzymatic assistance is involved.

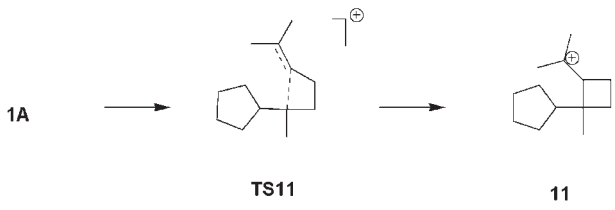

SCHEME 7. Formation of carbocation **11** with the pendant cyclobutyl ring.

Conclusion

The preliminary results also suggest that, to make a more complete search, many other rearrangement mechanisms of model cyclopentylheptenyl carbocations **1A** and **1B** are to be considered. As well, all B3LYP results are to be combined with results obtained at higher levels of theory, such as MP*n*, which can differently address electron correlation effects [20]. These effects are of special importance for structures with hypercoordinated hydrogens involved in three-center two electron C—H—C bonds.

This study has shown five competitive rearrangements in cyclopentylheptenyl type carbocations that were omitted from earlier discussions. These distinct alternative processes are related to

experimental findings already reported. A number of new intermediates and transition state structures were located along the corresponding reaction pathways (Figs. 1 and 2). The calculated energies of these stationary points allowed us to perform a comparative study of all five rearrangements. The rearrangement of **1B** which involves spiro-type intermediates (Scheme 4) is, both thermodynamically and kinetically, the most favorable process, whereas the rearrangement of **1B** which involves protonated cyclopropane intermediates (Scheme 6) is energetically the least feasible process.

ACKNOWLEDGMENTS

The author thanks the Computing Center of the University of Zagreb SRCE for allocating computer time on the Isabella cluster. A helpful discussion as well as cooperation with Danijel Ljubas is gratefully acknowledged.

References

1. (a) Abe, L.; Rohmer, M.; Restwich, G. D. Chem Rev 1993, 93, 2189; (b) Wendt, K. U.; Schulz, G. E.; Corey, E. J.; Liu, D. R. Angew Chem Int Ed 2000, 39, 2812.
2. (a) Nishizawa, M.; Takenaka, H.; Hayashi, Y. J Am Chem Soc 1985, 107, 522; (b) Corey, E. J.; Virgil, S. C.; Cheng, H.; Baker, C. H.; Matsuda, S. P. T.; Singh, V.; Sarshar, S. J Am Chem Soc 1995, 117, 11819; (c) Corey, E. J.; Cheng, H. Tetrahedron Lett 1996, 37, 2709.
3. (a) Jenson, C.; Jorgensen, W. L. J Am Chem Soc 1997, 119, 10846; (b) Rajamnai, R.; Gao, J. J Am Chem Soc 2003, 125, 12768; (c) Hess, B. A., Jr. Org Lett 2003, 5, 165; (d) Nishizawa, M.; Yadav, A.; Imagawa, H.; Sugihara, T. Tetrahedron Lett 2003, 44, 3867; (e) Matsuda, S. P. T.; Wilson, W. K.; Xiong, Q. Org Biomol Chem 2006, 4, 530.
4. Hess, B. A., Jr. J Am Chem Soc 2002, 124, 10286.
5. Vrcek, V. (manuscript in preparation).
6. (a) Vrcek, V.; Siehl, H.-U.; Kronja, O. J Phys Org Chem 2000, 13, 616; (b) Siehl, H.-U.; Vrcek, V.; Kronja, O. J Chem Soc Perkin Trans 2, 2002, 106; (c) Vrcek, V.; Saunders, M.; Kronja, O. J Org Chem 2003, 68, 1859.
7. Vrcek, V.; Vinkovic Vrcek, I; Kronja, O. Croat Chem Acta 2001, 74, 801.
8. Vrcek, V.; Vinkovic Vrcek, I; Siehl, H.-U. J Phys Chem A 2006, 110, 1868.
9. Frisch, M. J.; Trucks, G. W.; Schlegel, H. B.; Scuseria, G. E.; Robb, M. A.; Cheeseman, J. R.; Montgomery, J. A., Jr.; Vreven, T.; Kudin, K. N.; Burant, J. C.; Millam, J. M.; Iyengar, S. S.; Tomasi, J.; Barone, V.; Mennucci, B.; Cossi, M.; Scalmani, G.; Rega, N.; Petersson, G. A.; Nakatsuji, H.; Hada, M.; Ehara, M.; Toyota, K.; Fukuda, R.; Hasegawa, J.; Ishida, M.; Nakajima, T.; Honda, Y.; Kitao, O.; Nakai, H.; Klene, M.; Li, X.; Knox, J. E.; Hratchian, H. P.; Cross, J. B.; Adamo, C.; Jaramillo, J.; Gomperts, R.; Stratmann, R. E.; Yazyev, O.; Austin, A. J.; Cammi, R.; Pomelli, C.; Ochterski, J. W.; Ayala, P. Y.; Morokuma, K.; Voth, G. A.; Salvador, P.; Dannenberg, J. J.; Zakrzewski, V. G.; Dapprich, S.; Daniels, A. D.; Strain, M. C.; Farkas, O.; Malick, D. K.; Rabuck, A. D.; Raghavachari, K.; Foresman, J. B.; Ortiz, J. V.; Cui, Q.; Baboul, A. G.; Clifford, S.; Cioslowski, J.; Stefanov, B. B.; Liu, G.; Liashenko, A.; Piskorz, P.; Komaromi, I.; Martin, R. L.; Fox, D. J.; Keith, T.; Al-Laham, M. A.; Peng, C. Y.; Nanayakkara, A.; Challacombe, M.; Gill, P. M. W.; Johnson, B.; Chen, W.; Wong, M. W.; Gonzalez, C.; Pople, J. A. Gaussian 03; Revision C.02; Gaussian: Wallingford, CT, 2004.
10. (a) Lee, C.; Yang, W.; Parr, R. G. Phys Rev B 1988, 37, 785; (b) Becke, A. D. J Chem Phys 1993, 98, 5648; (c) Stevens, P. J.; Devlin, F. J.; Chablowski, C. F.; Frisch, M. J. J Chem Phys 1994, 98, 11623.
11. Gonzales, C.; Schlegel, H. B. J Phys Chem 1990, 94, 5523.
12. Epstein, W. W.; Grua, J. R.; Gregonis, D. J Org Chem 1982, 47, 1128.
13. (a) van Tamelen, E. E.; Willett, J. D.; Schwartz, M.; Nadeau, R. J Am Chem Soc 1966, 88, 5937; (b) van Tamelen, E. E.; Willett, J. D.; Clayton, R. B. J Am Chem Soc 1967, 89, 3371.
14. van Tamelen, E. E. J Am Chem Soc 1982, 104, 6480.
15. van Tamelen, E. E.; Lees, R. G.; Grieder, A. J Am Chem Soc 1974, 96, 2255.
16. (a) Vinkovic Vrcek, I; Vrcek, V.; Siehl, H.-U. J Phys Chem A 2002, 106, 1604; (b) Bojin, M. D.; Tantillo, D. J. J Phys Chem A 2006, 110, 4810.
17. (a) Fouillet, C. C. J.; Mareda, J. J Mol Struct (Theochem) 2002, 589, 7; (b) Li, T.; Janda, K. D.; Lerner, R. A. Nature 1996, 379, 326.
18. Lee, J. K.; Houk, K. N. Angew Chem Int Ed 1997, 36, 1003.
19. (a) Corey, E. J.; Virgil S. C.; Liu, D. R; Sarshar, S. J Am Chem Soc 1992, 114, 1524; (b) Corey, E. J.; de Montellano P. R. O.; Yamamoto, H. J Am Chem Soc 1968, 90, 6254.
20. (a) Schleyer, P. v. R.; Maerker, C. Pure Appl Chem 1995, 67, 755; (b) Schleyer, P. v. R.; Maerker, C.; Buzek, P.; Sieber, S. Stable Carbocations; Prakash, G. K. S.; Schleyer, P. v. R., Eds.; Wiley: New York, 1997; Chapter 2.